

Two-way relay networks with wireless power transfer: design and performance analysis

ISSN 1751-8628

Received on 16th August 2015

Revised on 29th February 2016

Accepted on 14th June 2016

doi: 10.1049/iet-com.2015.0728

www.ietdl.org

Yuanwei Liu¹ ✉, Lifeng Wang¹, Maged El Kashlan¹, Trung Q. Duong^{2,3}, Arumugam Nallanathan⁴

¹Electronic Engineering and Computer Science School, Queen Mary University of London, London, UK

²Electronic Engineering Department, Queen's University Belfast, Belfast, UK

³Duy Tan University, Vietnam

⁴Electronic Engineering Department, King's College London, London, UK

✉ E-mail: yuanwei.liu@qmul.ac.uk

Abstract: This study considers amplify-and-forward two-way relay networks, where an energy constrained relay node harvests energy from the received radio-frequency signal. Based on time switching receiver, they separate the energy harvesting (EH) phase and the information processing (IP) phase in time. In the EH phase, three practical wireless power transfer policies are proposed: (i) dual-source (DS) power transfer, where both sources transfer power to the relay; (ii) single-fixed-source power transfer, where a fixed source transfers power to the relay; and (iii) single-best-source (SBS) power transfer, where a source with the strongest channel transfers power to the relay. In the IP phase, a new comparative framework of the proposed wireless power transfer policies is presented in two bi-directional relaying protocols, known as multiple access broadcast (MABC) and time division broadcast (TDBC). To characterise the performance of the proposed policies, new analytical expressions are derived for the outage probability, the throughput, and the system energy efficiency. Numerical results corroborate the authors' analysis and show: (i) the DS policy performs the best in terms of both outage probability and throughput among the proposed policies, (ii) the TDBC protocol achieves lower outage probability than the MABC protocol, and (iii) there exists an optimal value of EH time fraction to maximise the throughput.

1 Introduction

Energy harvesting (EH) is an effective means to prolong the life of a wireless network, and has recently received remarkable attention. The recent research has shown that ambient radio-frequency (RF) signals are a new promising source for harvesting energy [1, 2]. The motivation behind this approach lies in the fact that most devices are surrounded by RF signals, and potentially, energy and information can be carried together by the RF signals during transmission. As a consequence, a new EH solution, which can achieve simultaneous wireless information and power transfer (SWIPT), was initially proposed [3]. Inspired by this concept, two practically realisable receiver designs, namely time switching (TS) receiver and power splitting (PS) receiver, were proposed for a multiple-input multiple-output wireless broadcast system to enable SWIPT [4]. The recent state-of-the-art research on SWIPT mainly focuses on practical receiver designs [4–8]. The work in [4] was extended in [5] by considering imperfect channel state information at the transmitter. Based on TS receiver, the secure device-to-device communication in cognitive radio networks was investigated with invoking a wireless power transfer model [6]. Moreover, with the aid of compressive sensing and matrix completion, the throughput of wireless powered cognitive radio networks was analysed in [7]. Based on PS receiver, in [8], an optimal PS rule at the receiver was derived to achieve tradeoffs for outage/energy as well as rate/energy both in delay-limited and delay-tolerant transmission modes.

The aforementioned literature on EH all considered the point-to-point system. For cooperative systems, the recent research works about SWIPT are based on two common relay protocols, namely, amplify-and-forward (AF) relay protocol and decode-and-forward (DF) relay protocol [9–11]. For the AF relay system, a TS-based relaying protocol and a PS-based relaying protocol were proposed to harvest energy from the received RF

signal at the energy constrained relay [9]. For the DF relay system with SWIPT, a novel wireless EH DF relaying protocol was proposed in [10] for underlay cognitive networks to enable secondary users can harvest energy from the primary users. Furthermore, a cooperative SWIPT non-orthogonal multiple access protocol was proposed in [11]. Due to the loss of spectral efficiency induced by one-way relaying, two-way relaying which can complete the information exchange within two time slots was proposed in [12]. Moreover, in order to enhance the transmission reliability in two-way relay networks (TWRNs), the comparison of a multiple access broadcast (MABC) protocol and a time division broadcast (TDBC) protocol were investigated in [13]. Based on the PS receiver, a two time-slot two-way relaying protocol, facilitating EH phase and IP phase simultaneously was analysed in [14] to apply EH in TWRNs.

The principal challenges in TWRN with wireless power transfer to an energy constrained relay are: (i) to improve the energy efficiency of the power transfer from the sources to the relay; and (ii) to enhance transmission reliability and throughput among all the nodes. Motivated by these two challenges, we propose three practical policies to efficiently transfer power with two protocols to reliably process information in TWRN with an energy constrained relay. Different from the aforementioned work [14], this paper presents a new comparative framework for MABC and TDBC protocols based on the TS receiver. As the extension of [15] which only considers the throughput, this work further considers outage probability and energy efficiency. The primary contributions of our paper are summarised as follows:

- In the EH phase, we propose the DS, SFS, and SBS power transfer policies to harvest energy at the energy constrained relay node. In the IP phase, we present a new comparative framework for each of the three wireless power transfer policies in two bi-directional relaying protocols, namely MABC and TDBC protocols.

- We derive new analytical expressions for each of the DS, SFS, and SBS policies in MABC and TDBC by evaluating: (i) the outage probability; (ii) the throughput both in the delay-limited transmission mode and delay-tolerant transmission mode; and (iii) the system energy efficiency both in the delay-limited transmission mode and the delay-tolerant transmission mode.
- Comparing the DS, SFS, and SBS policies, our results show: (i) the DS policy performs the best both in terms of outage probability and throughput; and (ii) the SBS is the most energy efficient policy. It is worth noting that the SBS policy offers an optimal tradeoff between performance and power.
- Comparing the MABC and TDBC, our results show: (i) the outage probability of TDBC is lower than that of MABC since TDBC has diversity gain; and (ii) there exists an optimal EH time fraction value for each of the proposed policies in MABC and TDBC protocols to achieve the maximum throughput.

2 System model

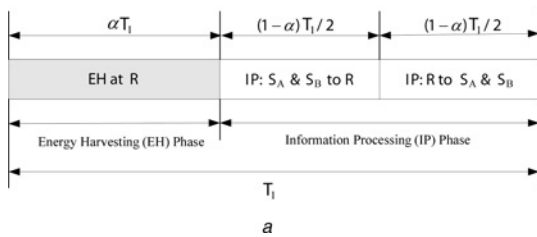
We consider a half-duplex TWRN, where the exchange of information between two single-antenna sources S_A and S_B is facilitated by an energy constrained intermediate AF relay R with a single antenna. Based on the TS receiver, we separate the EH and the IP phases in time, i.e. during the EH phase, the relay harvests energy from the source signals with wireless power transfer, and during the IP phase, the relay forwards information using the harvested energy. We consider MABC and TDBC protocols in the IP phase. All the channels are modelled as quasi-static block Rayleigh fading channels which means the channel condition remains unchanged in a frame. We denote h_{AR} , h_{BR} , and h_{AB} as the channel coefficients of $S_A \rightarrow R$, $S_B \rightarrow R$, and $S_A \rightarrow S_B$ links, respectively. The channel power gains $|h_{AR}|^2$, $|h_{BR}|^2$, and $|h_{AB}|^2$ are exponentially distributed random variables with the means $\Omega_A = K(d_{AR})^{-\zeta}$, $\Omega_B = K(d_{BR})^{-\zeta}$, and $\Omega_C = K(d_{AB})^{-\zeta}$, respectively, where K is a frequency dependent constant, d_{AR} , d_{BR} , and d_{AB} denote the distances of $S_A \rightarrow R$, $S_B \rightarrow R$, and $S_A \rightarrow S_B$ links, respectively, and ζ represents the path-loss exponent.

2.1 Multiple access broadcast

In this protocol, besides the time in the EH phase, two time slots are required in the IP phase. As shown in Fig. 1a, we denote the transmission time for one frame as T_1 . α is the fraction of time that the relay harvests energy from the source signals, where $0 < \alpha < 1$. The beginning αT_1 block time is the EH time, and the remaining $(1-\alpha)T_1$ block time is the IP time. Since the information length from sources to relay and relay to sources are identical, each of them will occupy $(1-\alpha)T_1/2$ time. In the first slot of the IP phase, both S_A and S_B transmit signals to R simultaneously with analogue network coding. Then the relay amplifies the mixed signals to the two sources in the second broadcast slot.

Consider the first slot, the signal received at R can be expressed as

$$y_R = \sqrt{P_A}h_{AR}x_A + \sqrt{P_B}h_{BR}x_B + n^{(R)}, \quad (1)$$



where $n^{(R)}$ is denoted as the additive white Gaussian noise (AWGN) at the relay R with variance σ_R^2 .

In the second time slot, the relay R amplifies the signal with a scaling gain and forwards the scaled signal to S_A and S_B with transmit power P_R , which depends on the amount of energy harvested during the energy harvest time. The received signal at S_i ($i \in (A, B)$) is given by

$$y_i = G_1 \sqrt{P_R} h_{iR} y_R + n^{(i)}, \quad (2)$$

where $i \in (A, B)$, $G_1 = (P_A |h_{AR}|^2 + P_B |h_{BR}|^2 + \sigma_R^2)^{-(1/2)}$ is the scaling gain based on the rules of variable gain AF relaying, and $n^{(i)}$ is the AWGN with variance σ_i^2 . Substituting (1) into (2), after subtracting self-interference at S_i , the signal is given by

$$\tilde{y}_i = G_1 \sqrt{P_R P_j} h_{iR} h_{jR} x_j + G_1 \sqrt{P_R} h_{iR} n^{(R)} + n^{(i)}, \quad (3)$$

where $(i, j) \in \{(A, B), (B, A)\}$, we denote P_A and P_B as the transmit powers at S_A and S_B , respectively. The relay's transmit power P_R depends on the amount of energy harvested during the energy harvest time and will be detailed in Section 3. Assuming that all the nodes have the same noise level with the variance σ^2 ($\sigma_A^2 = \sigma_B^2 = \sigma_R^2 = \sigma^2$), the end-to-end signal-to-noise ratio (SNR) at S_i is given by

$$\gamma_i = \frac{G_1^2 P_R P_j |h_{iR}|^2 |h_{jR}|^2}{G_1^2 P_R |h_{iR}|^2 \sigma^2 + \sigma^2}, \quad (4)$$

where $(i, j) \in \{(A, B), (B, A)\}$.

2.2 Time division broadcast

In this protocol, besides the time in the EH phase, three time slots are required in the IP phase. As shown in Fig. 1b, we denote the transmission time for one frame as T_2 . The beginning αT_2 block time is the EH time, and the remaining $(1-\alpha)T_2$ block time is the IP time. During the IP phase, each time slot will occupy $(1-\alpha)T_2/3$. In the first two slots of IP phase, S_A and S_B transmit information to relay R separately by time, then the relay amplifies the mixed signals to the two sources in the third broadcast slot.

Consider the first two time slots, the received signals of S_i and S_j through the direct-path link are denoted as

$$y_{i,1} = \sqrt{P_j} h_{AB} x_j + n_1^{(i)}, \quad y_{j,2} = \sqrt{P_i} h_{AB} x_i + n_2^{(j)}, \quad (5)$$

respectively, where $(i, j) \in \{(A, B), (B, A)\}$, $n_1^{(i)}$ and $n_2^{(j)}$ denote the AWGNs at S_i and S_j in the first and second slots with variances σ_i^2 and σ_j^2 , respectively.

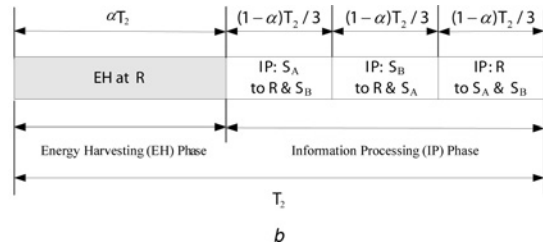


Fig. 1 Frame structures of EH for MABC and TDBC protocols

a MABC protocol
b TDBC protocol

For the relay link, the received signals at the relay node after the first two time slots are denoted as

$$y_{R,1} = \sqrt{P_j} h_{jR} x_j + n_1^{(R)}, \quad y_{R,2} = \sqrt{P_i} h_{iR} x_i + n_2^{(R)}, \quad (6)$$

respectively, where $(i, j) \in \{(A, B), (B, A)\}$, $n_1^{(R)}$ and $n_2^{(R)}$ denote the AWGNs at R in the first and second slots with variance σ_R^2 , respectively.

In the third time slot, the relay R amplifies the signal with a scaling gain and forwards the scaled signal to S_A and S_B with transmit power P_R , which depends on the amount of energy harvested during the energy harvest time. The received signal at source S_i can be expressed as

$$y_{i,3} = G_2 \sqrt{P_R} h_{iR} (y_{R,1} + y_{R,2}) + n_3^{(i)}, \quad (7)$$

where $i \in \{A, B\}$, $G_2 = (P_A |h_{AR}|^2 + P_B |h_{BR}|^2 + 2\sigma_R^2)^{-1/2}$ is the scaling gain based on the rules of variable gain AF relaying, and $n_3^{(i)}$ denotes the AWGN at S_i in the third slot with variance σ_i^2 . Substituting (6) into (7), and after subtracting self-interference at S_i , the signal is given by

$$\tilde{y}_{i,3} = G_2 \sqrt{P_R} h_{iR} h_{jR} x_j + G_2 \sqrt{P_R} h_{iR} (n_1^{(R)} + n_2^{(R)}) + n_3^{(i)}, \quad (8)$$

where $(i, j) \in \{(A, B), (B, A)\}$. Here, the relay's transmit power P_R depends on the amount of energy harvested during the energy harvest time and will be detailed in Section 3.

Each source utilises maximal radio combining (MRC) to combine the signals from the relay link and the direct link. Assuming that all the nodes have the same noise level with the variance σ^2 ($\sigma_A^2 = \sigma_B^2 = \sigma_R^2 = \sigma^2$), the received SNR after MRC at S_i is given by

$$\gamma_i^{\text{MRC}} = \frac{G_2^2 P_R P_j |h_{iR}|^2 |h_{jR}|^2}{G_2^2 P_R |h_{iR}|^2 2\sigma^2 + \sigma^2} + \frac{P_j |h_{AB}|^2}{\sigma^2}, \quad (9)$$

where $(i, j) \in \{(A, B), (B, A)\}$.

3 Wireless power transfer policies design and performance analysis

In this section, based on the TS receiver, three wireless power transfer policies, i.e. the DS policy, the SFS policy and the SBS policy are proposed in the EH phase. The MABC and TDBC transmission protocols are considered in the IP phase. In an effort to assess the proposed policies, we derive the compact expressions for principal performance metrics such as outage probability, throughput and system energy efficiency.

3.1 DS power transfer policy for MABC

In this subsection, we consider the DS policy for MABC.

(i) *End-to-end SNR*: In this policy, both S_A and S_B transfer power to the relay simultaneously, and the energy harvested at the relay can be expressed as

$$E_h = \eta(P_A |h_{AR}|^2 + P_B |h_{BR}|^2) \alpha T_1, \quad (10)$$

where $0 < \eta \leq 1$ is the energy conversion efficiency which depends on the EH circuit [16]. Based on (10), the transmit power at the relay is given by

$$P_R = \frac{E_h}{(1 - \alpha)T_1/2} = \frac{2\eta(P_A |h_{AR}|^2 + P_B |h_{BR}|^2) \alpha}{(1 - \alpha)}. \quad (11)$$

Substituting (11) into (4), we obtain a tight high SNR approximation for the end-to-end SNR at S_i as [9, 17]

$$\gamma_i = \frac{\varpi_j X Y}{\vartheta X + 1}, \quad (12)$$

where $(i, j) \in \{(A, B), (B, A)\}$, $\varpi_j = (P_j 2\eta\alpha/\sigma^2(1 - \alpha))$, $\vartheta = (2\eta\alpha/(1 - \alpha))$, $X = |h_{iR}|^2$, and $Y = |h_{jR}|^2$.

Lemma 1: We provide a unified approach to derive the cumulative distribution function (CDF) of γ_i as

$$F_{\gamma_i}(\gamma) = 1 - \frac{2e^{-(\gamma\vartheta/\Omega_j\varpi_j)}}{\Omega_i} \sqrt{\frac{\gamma\Omega_i}{\varpi_j\Omega_j}} K_1 \left(2\sqrt{\frac{\gamma}{\varpi_j\Omega_i\Omega_j}} \right), \quad (13)$$

where $(i, j) \in \{(A, B), (B, A)\}$, $K_n(\cdot)$ is the n th order modified Bessel function of the second kind.

Proof: The CDF of γ_i is expressed as

$$\begin{aligned} F_{\gamma_i}(\gamma) &= \Pr \left[Y \leq \frac{\gamma(\vartheta X + 1)}{\varpi_j X} \right] \\ &= 1 - \frac{e^{-(\gamma\vartheta/\Omega_j\varpi_j)}}{\Omega_i} \int_0^\infty e^{-(\gamma/\Omega_j\varpi_j y) - (y/\Omega_i)} dy. \end{aligned} \quad (14)$$

Using [18, Eq. (3.324.1)], we obtain the desired result in (13). \square

(ii) *Outage probability*: We first characterise the performance in terms of the outage probability. In TWRN, the network is defined as in outage if either the transmission from source A to source B or from source B to source A is in outage. Thus, the probability of TWRN is defined as

$$\begin{aligned} P_{\text{out}} &= \Pr(R_A \leq R_A^0, \quad \text{or} \quad R_B \leq R_B^0) \\ &= \Pr(\gamma_A < \gamma_A^0) + \Pr(\gamma_B < \gamma_B^0) - \Pr(\gamma_A < \gamma_A^0, \gamma_B < \gamma_B^0), \end{aligned} \quad (15)$$

where $\gamma_i^0 = 2^{2R_i^0} - 1$ for $i \in \{A, B\}$, with γ_A^0 is the threshold at S_A and γ_B^0 is the threshold at S_B .

Following (15) and using Lemma 1, the outage probability of the DS policy for MABC is given by

$$P_{\text{out}}^{\text{DS-MABC}} = P_{\text{out}}^A + P_{\text{out}}^B - P_{\text{out}}^{AB}, \quad (16)$$

where $P_{\text{out}}^A \triangleq F_{\gamma_A}(\gamma_A^0)$, $P_{\text{out}}^B \triangleq F_{\gamma_B}(\gamma_B^0)$, and $P_{\text{out}}^{AB} \triangleq F_{\gamma_A, \gamma_B}(\gamma_A^0, \gamma_B^0)$, $F_{\gamma_A}(\gamma_A^0)$ and $F_{\gamma_B}(\gamma_B^0)$ are given in (13), $F_{\gamma_A, \gamma_B}(\gamma_A^0, \gamma_B^0)$ is provided in Appendix 1 with $\varpi_A = (P_A 2\eta\alpha/\sigma^2(1 - \alpha))$, $\varpi_B = (P_B 2\eta\alpha/\sigma^2(1 - \alpha))$, and $\vartheta = (2\eta\alpha/(1 - \alpha))$.

(iii) *Throughput analysis*: We now derive the throughput in two different transmission modes, i.e. delay-limited and delay-tolerant.

(a) *Delay-limited Transmission*: In delay-limited transmission, the source transmits information at a fixed rate and outage probability plays a pivotal role in the throughput. Given that S_A and S_B transmit information with fixed rates R_A^0 and R_B^0 bits/s/Hz, respectively, where $R_A^0 \triangleq \log_2(1 + \gamma_A^0)$ and $R_B^0 \triangleq \log_2(1 + \gamma_B^0)$, the throughput is calculated as

$$\tau_l = \frac{(1 - \alpha)T_1/2}{T_1} ((1 - P_{\text{out}}^A)R_A^0 + (1 - P_{\text{out}}^B)R_B^0), \quad (17)$$

where $P_{\text{out}}^A \triangleq F_{\gamma_A}(\gamma_A^0)$ is the outage probability at S_A and $P_{\text{out}}^B \triangleq F_{\gamma_B}(\gamma_B^0)$ is the outage probability at S_B , with $F_{\gamma_A}(\gamma_A^0)$ and $F_{\gamma_B}(\gamma_B^0)$ given in (13).

(b) *Delay-tolerant transmission*: In delay-tolerant transmission, the throughput is determined by evaluating the ergodic rate. Using (13), the throughput is calculated as

$$\begin{aligned}\tau_t &= \frac{(1-\alpha)T_1/2}{T_1} (\mathbb{E}\{\log_2(1+\gamma_A)\} + \mathbb{E}\{\log_2(1+\gamma_B)\}) \\ &= \frac{1-\alpha}{2\ln 2} \int_0^\infty \ln(1+x) f_{\gamma_A}(x) dx + \frac{1-\alpha}{2\ln 2} \int_0^\infty \ln(1+y) f_{\gamma_B}(y) dy \\ &\stackrel{(a)}{=} \frac{1-\alpha}{2\ln 2} \left(\int_0^\infty \frac{1-F_{\gamma_A}(\lambda)}{1+\lambda} d\lambda + \int_0^\infty \frac{1-F_{\gamma_B}(\lambda)}{1+\lambda} d\lambda \right) \\ &= \frac{1-\alpha}{\ln 2} \sum_{\{i,j\} \in \{A,B\}} \int_0^\infty \frac{\sqrt{(\lambda/\varpi_j \Omega_i \Omega_j)} K_1(2\sqrt{(\lambda/\varpi_j \Omega_i \Omega_j)})}{(1+\lambda)e^{(\lambda\vartheta/\Omega_j \varpi_j)}} d\lambda,\end{aligned}\quad (18)$$

where $\mathbb{E}\{\cdot\}$ is the expectation operator and (a) is obtained by using the partial integration.

(iv) *System energy efficiency*: Based on throughput analysis, we proceed to examine the system energy efficiency considering different wireless power transfer policies in the EH phase and different information transmission protocols in the IP phase. The definition of energy efficiency is given by

$$\bar{\eta}^{EE} = \frac{\text{Total amount of data delivered}}{\text{Total energy consumed}}. \quad (19)$$

For the TWRN system energy efficiency, the total amount of data delivered is denoted as the sum throughput from S_A to S_B and from S_B to S_A via the energy constrained relay R . The total power consumed is denoted as the sum of the transmit power P_A at S_A and P_B at S_B , both including the power consumed in the EH phase and the IP phase. Since the relay's transmit power P_R depends on the amount of energy harvested during the EH phase, the relay does not cost extra energy. Based on throughput analysis in Section 3.1(iii), the system energy efficiency for the DS policy in the MABC protocol is expressed as

$$\bar{\eta}_\Phi^{EE} = \frac{\tau_\Phi}{(1/2)(P_A + P_B)(1+\alpha)}, \quad (20)$$

where $\Phi \in (l, t)$. $\bar{\eta}_l^{EE}$ is the system energy efficiency in delay-limited transmission mode and $\bar{\eta}_t^{EE}$ is the system energy efficiency in delay-tolerant transmission mode.

3.2 DS power transfer policy for TDBC

In this subsection, we consider the DS policy for TDBC.

(i) *End-to-end SNR*: As suggested in Section 3.1(i), the energy harvested at the relay can be expressed as

$$E_h = \eta(P_A |h_{AR}|^2 + P_B |h_{BR}|^2) \alpha T_2. \quad (21)$$

Based on (21), the transmit power at the relay is given by

$$P_R = \frac{E_h}{(1-\alpha)T_2/3} = \frac{3\eta\alpha(P_A |h_{AR}|^2 + P_B |h_{BR}|^2)}{(1-\alpha)}. \quad (22)$$

Substituting (22) into (9), we obtain a tight high SNR approximation for the end-to-end SNR at S_i as

$$\gamma_i^{\text{MRC}} = \frac{\varpi_j XY}{\vartheta X + 1} + \Psi_j Z, \quad (23)$$

where $(i, j) \in \{(A, B), (B, A)\}$, $\varpi_j = (3\eta\alpha P_j / \sigma^2(1-\alpha))$, $\vartheta = (6\eta\alpha / (1-\alpha))$, $X = |h_{iR}|^2$, $Y = |h_{jR}|^2$, $\Psi_j = (P_j / \sigma^2)$, and $Z = |h_{AB}|^2$.

Lemma 2: The CDF of γ_i^{MRC} is

$$\begin{aligned}F_{\gamma_i^{\text{MRC}}}(\gamma) &= 1 - e^{-(\gamma/\Psi_j \Omega_C)} \\ &\quad - a_1 e^{b_1 \gamma} \int_0^{\sqrt{\gamma}} e^{-c_1 \lambda^2} \lambda^2 K_1(t_1 \lambda) d\lambda,\end{aligned}\quad (24)$$

where

$$\begin{aligned}(i, j) &\in \{(A, B), (B, A)\}, \quad a_1 = \frac{4}{\Omega_C \Psi_j} \sqrt{\frac{1}{\varpi_j \Omega_i \Omega_j}}, \\ b_1 &= -\frac{1}{\Omega_C \Psi_j}, \quad c_1 = \left(\frac{\vartheta}{\Omega_j \varpi_j} - \frac{1}{\Omega_C \Psi_j} \right), \quad \text{and} \quad t_1 = \sqrt{\frac{4}{\varpi_j \Omega_i \Omega_j}}.\end{aligned}$$

Proof: The CDF of γ_i^{MRC} is expressed as

$$F_{\gamma_i^{\text{MRC}}}(\gamma) = \Pr \left[\frac{\varpi_j XY}{\vartheta X + 1} + \Psi_j Z \leq \gamma \right] \quad (25)$$

With the help of (13), we can obtain the result in (24). \square

(ii) *Outage probability*:

Lemma 3: The joint distribution function of $F_{\gamma_A^{\text{MRC}}, \gamma_B^{\text{MRC}}}$ for the DS policy in the TDBC protocol can be expressed as

$$\begin{aligned}F_{\gamma_A^{\text{MRC}}, \gamma_B^{\text{MRC}}}(\gamma_A, \gamma_B) &= \int_0^{\min\{(\gamma_A/\Psi_A), (\gamma_B/\Psi_B)\}} F_{\gamma_A, \gamma_B}(\gamma_A - \Psi_B z, \gamma_B - \Psi_A z) \frac{e^{-(z/\Omega_C)}}{\Omega_C} dz,\end{aligned}\quad (26)$$

where F_{γ_A, γ_B} is provided in Appendix 1 with $\varpi_A = (3\eta\alpha P_A / \sigma^2(1-\alpha))$, $\varpi_B = (3\eta\alpha P_B / \sigma^2(1-\alpha))$, and $\vartheta = (6\eta\alpha / (1-\alpha))$.

Using Lemmas 2 and 3, following (15), the outage probability of the DS policy for TDBC is given by

$$P_{\text{out}}^{\text{DS-TDBC}} = P_{\text{out}}^A + P_{\text{out}}^B - P_{\text{out}}^{AB}, \quad (27)$$

where $P_{\text{out}}^A \triangleq F_{\gamma_A^{\text{MRC}}}(\gamma_A^0)$, $P_{\text{out}}^B \triangleq F_{\gamma_B^{\text{MRC}}}(\gamma_B^0)$, and $P_{\text{out}}^{AB} \triangleq F_{\gamma_A^{\text{MRC}}, \gamma_B^{\text{MRC}}}(\gamma_A^0, \gamma_B^0)$. Here, $F_{\gamma_A^{\text{MRC}}}(\gamma_A^0)$ and $F_{\gamma_B^{\text{MRC}}}(\gamma_B^0)$ are given in (24), $F_{\gamma_A^{\text{MRC}}, \gamma_B^{\text{MRC}}}(\gamma_A^0, \gamma_B^0)$ is provided in (26).

(iii) *Throughput analysis*:

(a) *Delay-limited transmission*: As suggested in Section 3.1(iii), in delay-limited transmission, the throughput is calculated as

$$\tau_l = \frac{(1-\alpha)T_2/3}{T_2} ((1-P_{\text{out}}^A)R_A^0 + (1-P_{\text{out}}^B)R_B^0), \quad (28)$$

where $P_{\text{out}}^A \triangleq F_{\gamma_A^{\text{MRC}}}(\gamma_A^0)$ and $P_{\text{out}}^B \triangleq F_{\gamma_B^{\text{MRC}}}(\gamma_B^0)$, $F_{\gamma_A^{\text{MRC}}}(\gamma_A^0)$ and $F_{\gamma_B^{\text{MRC}}}(\gamma_B^0)$ are given in (24).

(b) *Delay-tolerant transmission*: In delay-tolerant transmission, using (24), the throughput is calculated as (see (29))

where $\text{Ei}(\cdot)$ is the exponential integral function [18, eq. (8.211.1)].

(iv) *System energy efficiency*: As suggested in Section 3.1(iv), based on the throughput analysis in Section 3.2(iii), the system energy efficiency for the DS policy in the TDBC protocol is expressed as

$$\bar{\eta}_{\Phi}^{\text{EE}} = \frac{\tau_{\Phi}}{(1/3)(P_A + P_B)(1 + 2\alpha)}, \quad (30)$$

where $\Phi \in (l, t)$.

3.3 SFS power transfer policy for MABC

In this subsection, we consider the SFS policy for MABC.

(i) *End-to-end SNR*: In this policy, only a fixed source S_A or S_B transfers power to the relay. Without loss of generality, we assume this source is S_A , the energy harvested at the relay can be expressed as

$$E_h = \eta P_A |h_{AR}|^2 \alpha T_1. \quad (31)$$

Based on (31), the transmit power at the relay is given by

$$P_R = \frac{E_h}{(1 - \alpha)T_1/2} = \frac{2\eta\alpha P_A |h_{AR}|^2}{(1 - \alpha)}. \quad (32)$$

Substituting (32) into (4), we obtain a tight high SNR approximations for the end-to-end SNR at S_A and S_B as

$$\gamma_A = \frac{a_2 \Psi_A \Psi_B X^2 Y}{b_2 \Psi_A X^2 + \Psi_B Y + \Psi_A X}, \quad (33)$$

and

$$\gamma_B = \frac{a_2 \Psi_A X^2 Y}{b_2 \Psi_A X Y + \Psi_A X + \Psi_B Y}, \quad (34)$$

respectively, where $X = |h_{AR}|^2$, $Y = |h_{BR}|^2$, $a_2 = (2\eta\alpha/(1 - \alpha))$, $b_2 = (2\eta\alpha/(1 - \alpha))$, $\Psi_A = (P_A/\sigma^2)$, and $\Psi_B = (P_B/\sigma^2)$.

Lemma 4: The CDF of γ_A in (33) is

$$F_{\gamma_A}(\gamma) = 1 - \frac{1}{\Omega_A} \int_{X_1}^{\infty} e^{-(((\gamma b_2 \Psi_A X^2 + \gamma \Psi_A X)/(\Omega_B (a_2 \Psi_A \Psi_B X^2 - \gamma \Psi_B Y))) + (x/\Omega_A))} dx, \quad (35)$$

with $X_1 = \sqrt{(\gamma/a_2 \Psi_A)}$, and the CDF of γ_B in (34) is

$$F_{\gamma_B}(\gamma) = 1 - \frac{1}{\Omega_A} \int_{X_2}^{\infty} e^{-(((\Psi_A X \gamma)/(\Omega_B (a_2 \Psi_A X^2 - b_2 \Psi_A X \gamma - \Psi_B \gamma))) + (x/\Omega_A))} dx, \quad (36)$$

with

$$X_2 = \frac{b_2 \gamma + \sqrt{(b_2 \gamma)^2 + 4a_2 \Psi_B \gamma}}{2a_2 \Psi_A}.$$

Proof: The proof is accomplished in the similar method as the proof of Lemma 1. \square

(ii) *Outage probability*: Using Lemma 4, following (15), the outage probability of the SFS policy for MABC is given by

$$P_{\text{out}}^{\text{SFS-MABC}} = P_{\text{out}}^A + P_{\text{out}}^B - P_{\text{out}}^{AB}, \quad (37)$$

where $P_{\text{out}}^A \triangleq F_{\gamma_A}(\gamma_A^0)$, $P_{\text{out}}^B \triangleq F_{\gamma_B}(\gamma_B^0)$, and $P_{\text{out}}^{AB} \triangleq F_{\gamma_A, \gamma_B}(\gamma_A^0, \gamma_B^0)$. Here, $F_{\gamma_A}(\gamma_A^0)$ and $F_{\gamma_B}(\gamma_B^0)$ are given in (35) and (36), respectively, and $F_{\gamma_A, \gamma_B}(\gamma_A^0, \gamma_B^0)$ is provided in Appendix 2.

iii. *Throughput analysis*:

(a) *Delay-limited transmission*: In this mode, the expression for the throughput is the same as (17), where $P_{\text{out}}^A \triangleq F_{\gamma_A}(\gamma_A^0)$ and $P_{\text{out}}^B \triangleq F_{\gamma_B}(\gamma_B^0)$, $F_{\gamma_A}(\gamma_A^0)$ and $F_{\gamma_B}(\gamma_B^0)$ are given in (35) and (36), respectively.

(b) *Delay-tolerant transmission*: In this mode, similar to (18), the throughput is calculated as

$$\tau_t = \frac{1 - \alpha}{2 \ln 2} \left(\int_0^{\infty} \frac{1 - F_{\gamma_A}(\lambda)}{1 + \lambda} d\lambda + \int_0^{\infty} \frac{1 - F_{\gamma_B}(\lambda)}{1 + \lambda} d\lambda \right), \quad (38)$$

where $F_{\gamma_A}(\lambda)$ and $F_{\gamma_B}(\lambda)$ are given in (35) and (36), respectively.

System energy efficiency: As suggested in Section 3.1(iv), based on throughput analysis in Section 3.3(iii), the system energy efficiency for the SFS policy in the MABC protocol is expressed as

$$\bar{\eta}_{\Phi}^{\text{EE}} = \frac{\tau_{\Phi}}{P_A \alpha + (1/2)(P_A + P_B)(1 - \alpha)}. \quad (39)$$

3.4 SFS power transfer policy for TDBC

In this subsection, we consider the SFS policy for TDBC.

(i) *End-to-end SNR*: As suggested in Section 3.3(i), the energy harvested at the relay can be expressed as

$$E_h = \eta P_A |h_{AR}|^2 \alpha T_2. \quad (40)$$

$$\tau_t = \frac{(1 - \alpha)T_2/3}{T_2} (\mathbb{E}\{\log_2(1 + \gamma_A)\} + \mathbb{E}\{\log_2(1 + \gamma_B)\}) = -\frac{1 - \alpha}{3 \ln 2} \sum_{\substack{\{i,j\} \in \{A,B\} \\ i \neq j}} \left(e^{-b_1} \text{Ei}(b_1) + a_1 e^{-b_1} \int_0^{\infty} (e^{-c_1 \lambda^2} \lambda^2 K_1(t_1 \lambda)) \text{Ei}((\lambda^2 + 1)b_1) d\lambda \right), \quad (29)$$

Based on (40), the transmit power at the relay is given by

$$P_R = \frac{E_h}{(1-\alpha)T_2/3} = \frac{3\eta\alpha P_A |h_{AR}|^2}{(1-\alpha)}. \quad (41)$$

Substituting (41) into (9), we obtain a tight high SNR approximations for the end-to-end SNR at S_A and S_B as

$$\gamma_A^{\text{MRC}} = \frac{a_3 \Psi_A \Psi_B X^2 Y}{b_3 \Psi_A X^2 + \Psi_B Y + \Psi_A X} + \Psi_B Z, \quad (42)$$

and

$$\gamma_B^{\text{MRC}} = \frac{a_3 \Psi_A^2 X^2 Y}{b_3 \Psi_A X Y + \Psi_A X + \Psi_B Y} + \Psi_A Z, \quad (43)$$

respectively, where $a_3 = (3\eta\alpha/(1-\alpha))$, $b_3 = (6\eta\alpha/(1-\alpha))$, $X = |h_{AR}|^2$, $Y = |h_{BR}|^2$, and $Z = |h_{AB}|^2$.

Lemma 5: The CDF of γ_A^{MRC} in (42) is (see (44))

with $X_1 = \sqrt{(\gamma_A(z)/a_3 \Psi_A)}$, and the CDF of γ_B^{MRC} in (43) is (see (45))

where

$$X_2 = \frac{b_3 \gamma_B(z) + \sqrt{(b_3 \gamma_B(z))^2 + 4a_3 \Psi_B \gamma_B(z)}}{2a_3 \Psi_A}$$

$$\gamma_A(z) = \gamma - \Psi_B z, \quad \text{and} \quad \gamma_B(z) = \gamma - \Psi_A z.$$

(ii) Outage probability:

Lemma 6: The joint distribution function of $F_{\gamma_A^{\text{MRC}}, \gamma_B^{\text{MRC}}}$ for the SFS policy in the TDBC protocol can be expressed as

$$F_{\gamma_A^{\text{MRC}}, \gamma_B^{\text{MRC}}}(Y_A, Y_B) = \int_0^{\min\{(Y_A/\Psi_A), (Y_B/\Psi_B)\}} F_{\gamma_A, \gamma_B}(Y_A - \Psi_B z, Y_B - \Psi_A z) \frac{e^{-(z/\Omega_C)}}{\Omega_C} dz, \quad (46)$$

where F_{γ_A, γ_B} is provided in Appendix 2, with interchanging the parameters $a_3 \rightarrow a_2$ and $b_3 \rightarrow b_2$.

Using Lemmas 5 and 6, following (15), the outage probability of the SFS policy for MABC is given by

$$P_{\text{out}}^{\text{SFS-TDBC}} = P_{\text{out}}^A + P_{\text{out}}^B - P_{\text{out}}^{AB}, \quad (47)$$

where $P_{\text{out}}^A \triangleq F_{\gamma_A^{\text{MRC}}}(\gamma_A^0)$, $P_{\text{out}}^B \triangleq F_{\gamma_B^{\text{MRC}}}(\gamma_B^0)$, and $P_{\text{out}}^{AB} \triangleq F_{\gamma_A^{\text{MRC}}, \gamma_B^{\text{MRC}}}(\gamma_A^0, \gamma_B^0)$. Here, $F_{\gamma_A^{\text{MRC}}}(\gamma_A^0)$, $F_{\gamma_B^{\text{MRC}}}(\gamma_B^0)$, and $F_{\gamma_A^{\text{MRC}}, \gamma_B^{\text{MRC}}}(\gamma_A^0, \gamma_B^0)$ are given in (44), (45), and (46), respectively.

(iii) Throughput analysis:

(a) *Delay-limited transmission:* In this mode, the expression for the throughput is the same as (28), where $P_{\text{out}}^A \triangleq F_{\gamma_A^{\text{MRC}}}(\gamma_A^0)$ and

$P_{\text{out}}^B \triangleq F_{\gamma_B^{\text{MRC}}}(\gamma_B^0)$, $F_{\gamma_A^{\text{MRC}}}(\gamma_A^0)$ and $F_{\gamma_B^{\text{MRC}}}(\gamma_B^0)$ are given in (44) and (45), respectively.

(b) *Delay-tolerant transmission:* In this mode, similar to (29), the throughput is calculated as

$$\tau_i = \frac{1-\alpha}{3 \ln 2} \times \left(\int_0^\infty \frac{1-F_{\gamma_A^{\text{MRC}}}(\gamma)}{1+\lambda} d\lambda + \int_0^\infty \frac{1-F_{\gamma_B^{\text{MRC}}}(\gamma)}{1+\lambda} d\lambda \right), \quad (48)$$

where $F_{\gamma_A^{\text{MRC}}}(\lambda)$ and $F_{\gamma_B^{\text{MRC}}}(\lambda)$ are given in (44) and (45), respectively.

(iv) *System energy efficiency:* As suggested in Section 3.1(iv), based on the throughput analysis in Section 3.4(iii), the system energy efficiency for the SFS policy in the TDBC protocol is expressed as

$$\bar{\eta}_{\Phi}^{\text{EE}} = \frac{\tau_{\Phi}}{P_A \alpha + (1/3)(P_A + P_B)(1-\alpha)}, \quad (49)$$

where $\Phi \in (l, t)$.

3.5 SBS power transfer policy for MABC

In this subsection, we consider the SBS policy for MABC.

(i) *End-to-end SNR:* In this policy, we select the strongest channel to transfer power to the relay, the energy harvested at the relay can be expressed as

$$E_h = \eta P_k \max\{|h_{AR}|^2, |h_{BR}|^2\} \alpha T_1, \quad (50)$$

where

$$P_k = \begin{cases} P_A, & |h_{AR}|^2 > |h_{BR}|^2 \\ P_B, & |h_{AR}|^2 < |h_{BR}|^2 \end{cases}$$

Based on (50), the transmit power at the relay is given by

$$P_R = \frac{E_h}{(1-\alpha)T_1/2} = \frac{2\eta\alpha P_k \max\{|h_{AR}|^2, |h_{BR}|^2\}}{(1-\alpha)}. \quad (51)$$

Substituting (51) into (4), we obtain a tight high SNR approximation for the end-to-end SNR at S_i as

$$\gamma_i = \frac{a_4 \Psi_k \Psi_j \max\{|h_{iR}|^2, |h_{jR}|^2\} |h_{iR}|^2 |h_{jR}|^2}{b_4 \Psi_k \max\{|h_{iR}|^2, |h_{jR}|^2\} |h_{iR}|^2 + \Psi_i |h_{iR}|^2 + \Psi_j |h_{jR}|^2}, \quad (52)$$

where $(i, j) \in \{(A, B), (B, A)\}$, $a_4 = (2\eta\alpha/(1-\alpha))$, $b_4 = (2\eta\alpha/(1-\alpha))$, $\Psi_i = (P_i/\sigma^2)$, $\Psi_j = (P_j/\sigma^2)$, and $\Psi_k = (P_k/\sigma^2)$.

Lemma 7: The CDF of γ_i in (52) is given by (53) at the top of this page (see equation (53) at the bottom of the next page)

$$F_{\gamma_A^{\text{MRC}}}(\gamma) = 1 - e^{-(\gamma/\Omega_C \Psi_B)} - \frac{1}{\Omega_A \Omega_C} \int_0^{(\gamma/\Psi_B)} \int_{X_1}^\infty e^{-((\gamma_A(z)(b_3 \Psi_A X^2 + \Psi_A X))/(\Omega_B(a_3 \Psi_A \Psi_B X^2 - \gamma_A(z) \Psi_B))) - (x/\Omega_A) - (z/\Omega_C)} dx dz, \quad (44)$$

$$F_{\gamma_B^{\text{MRC}}}(\gamma) = 1 - e^{-(\gamma/\Omega_C \Psi_A)} - \frac{1}{\Omega_A \Omega_C} \int_0^{(\gamma/\Psi_A)} \int_{X_2}^\infty e^{-((\Psi_A X \gamma_B(z))/(\Omega_B(a_3 \Psi_A^2 X^2 - \gamma_B(z)(b_3 \Psi_A X + \Psi_B)))) - (x/\Omega_A)} dx dz, \quad (45)$$

where $(i, j) \in \{(A, B), (B, A)\}$, where $U(x)$ is the unit step function with a jump discontinuity at $x=0$, i.e.(see (53))

Proof: The CDF in (52) can be expressed as

$$\begin{aligned} F_{\gamma_i}(\gamma) &= \Pr\left[\frac{a_4\Psi_k\Psi_j\max\{X, Y\}XY}{b_4\Psi_k\max\{X, Y\}X + \Psi_iX + \Psi_jY} \leq \gamma\right] \\ &= \Pr[X\Delta_1 \leq \Psi_jY\gamma, X \leq Y, \Delta_1 \geq 0] \\ &\quad + \Pr[Y\Delta_2 \leq b_4\Psi_kX^2\gamma + \Psi_i\gamma X, X > Y, \Delta_2 \geq 0] \\ &\quad + \Pr[X > Y, \Delta_2 < 0] + \Pr[X \leq Y, \Delta_1 < 0], \end{aligned} \quad (54)$$

where $\Delta_1 = a_4\Psi_j^2Y^2 - b_4\Psi_jY\gamma - \Psi_i\gamma$ and $\Delta_2 = a_4\Psi_i\Psi_jX^2 - \Psi_j\gamma$. Based on (54), we can obtain (53) in the similar method as the proof of Lemma 1. \square

(ii) *Outage probability:* Using Lemma 7, following (15), the outage probability of the SBS policy for MABC is given by

$$P_{\text{out}}^{\text{SBS-MABC}} = P_{\text{out}}^A + P_{\text{out}}^B - P_{\text{out}}^{AB}, \quad (55)$$

where $P_{\text{out}}^A \triangleq F_{\gamma_A}(\gamma_A^0)$, $P_{\text{out}}^B \triangleq F_{\gamma_B}(\gamma_B^0)$, and $P_{\text{out}}^{AB} \triangleq F_{\gamma_A, \gamma_B}(\gamma_A^0, \gamma_B^0)$. Here, $F_{\gamma_A}(\gamma_A^0)$ and $F_{\gamma_B}(\gamma_B^0)$ are given in (53) at the top of next page, and $F_{\gamma_A, \gamma_B}(\gamma_A^0, \gamma_B^0)$ is provided in Appendix 3.

(iii) *Throughput analysis:*

(a) *Delay-limited transmission:* In this mode, the expression for the throughput is the same as (17), where $P_{\text{out}}^A \triangleq F_{\gamma_A}(\gamma_A^0)$ and $P_{\text{out}}^B \triangleq F_{\gamma_B}(\gamma_B^0)$. Here, $F_{\gamma_A}(\gamma_A^0)$ and $F_{\gamma_B}(\gamma_B^0)$ are given in (53).

(b) *Delay-tolerant transmission:* In this mode, similar to (18), the throughput is calculated using (38) where $F_{\gamma_A}(\lambda)$ and $F_{\gamma_B}(\lambda)$ are given in (53).

(iv) *System energy efficiency:* As suggested in Section 3.1(iv), based on the throughput analysis in Section 3.5(iii), the system energy efficiency for the SBS policy in the MABC protocol is expressed as

$$\bar{\eta}_{\Phi}^{EE} = \frac{\tau_{\Phi}}{P_k\alpha + (1/2)(P_A + P_B)(1 - \alpha)}, \quad (56)$$

where $\Phi \in (l, t)$, and

$$P_k = \begin{cases} P_A, |h_{AR}|^2 \cdots |h_{BR}|^2 \\ P_B, |h_{AR}|^2 < |h_{BR}|^2 \end{cases}.$$

3.6 SBS power transfer policy for TDBC

In this subsection, we consider the SBS policy for TDBC.

(i) *End-to-end SNR:* As suggested in Section 3.5(i), the energy harvested at the relay can be expressed as

$$E_h = \eta P_k \max\{|h_{AR}|^2, |h_{BR}|^2\} \alpha T_2, \quad (57)$$

where

$$P_k = \begin{cases} P_A, |h_{AR}|^2 \cdots |h_{BR}|^2 \\ P_B, |h_{AR}|^2 < |h_{BR}|^2 \end{cases}.$$

Based on (57), the transmit power at the relay is given by

$$P_R = \frac{E_h}{(1 - \alpha)T_2/3} = \frac{3\eta\alpha P_k \max\{|h_{AR}|^2, |h_{BR}|^2\}}{(1 - \alpha)}. \quad (58)$$

Substituting (58) into (9), we obtain a tight high SNR approximation for the end-to-end SNR at S_i as

$$\gamma_i^{\text{MRC}} = \Psi_j |h_{AB}|^2 + \frac{a_5 \Psi_k \Psi_j \max\{|h_{iR}|^2, |h_{jR}|^2\} |h_{iR}|^2 |h_{jR}|^2}{b_5 \Psi_k \max\{|h_{iR}|^2, |h_{jR}|^2\} |h_{iR}|^2 + \Psi_i |h_{iR}|^2 + \Psi_j |h_{jR}|^2}, \quad (59)$$

where $(i, j) \in \{(A, B), (B, A)\}$, $a_5 = (3\eta\alpha/(1 - \alpha))$, $b_5 = (6\eta\alpha/(1 - \alpha))$, $\Psi_i = (P_i/\sigma^2)$, $\Psi_j = (P_j/\sigma^2)$, and $\Psi_k = (P_k/\sigma^2)$.

Lemma 8: The CDF of γ_i^{MRC} in (59) is

$$F_{\gamma_i^{\text{MRC}}}(\gamma) = \int_0^{(\gamma/\Psi_j)} F_{\gamma_i}(\gamma - \Psi_j z) \frac{e^{-(z/\Omega_C)}}{\Omega_C} dz, \quad (60)$$

where $(i, j) \in \{(A, B), (B, A)\}$, and F_{γ_i} is given in (53).

$$\begin{aligned} F_{\gamma_i}(\gamma) &= \int_{\max\{K_1, K_3\}}^{\infty} \chi_1(\kappa) d\kappa + \int_{\max\{K_2, K_4\}}^{\infty} \chi_2(\kappa) d\kappa + U(K_3 - K_1) \left(e^{-(K_1/\Omega_j)} - e^{-(K_3/\Omega_j)} - m_i \left(e^{-(K_1/m_i\Omega_j)} - e^{-(K_3/m_i\Omega_j)} \right) \right) \\ &\quad + U(K_4 - K_2) \left(e^{-(K_2/\Omega_i)} - e^{-(K_4/\Omega_i)} - m_j \left(e^{-(K_2/m_j\Omega_i)} - e^{-(K_4/m_j\Omega_i)} \right) \right) + 1 - e^{-(K_1/\Omega_j)} - e^{-(K_2/\Omega_i)} + m_i e^{-(K_1/m_i\Omega_j)} + m_j e^{-(K_2/m_j\Omega_i)}. \end{aligned} \quad (53)$$

$$U(x) = \begin{cases} 1, & x > 0 \\ 0, & x \leq 0 \end{cases}, \quad \chi_1(\kappa) = \frac{1}{\Omega_j} e^{-(\kappa/\Omega_j)} - \frac{1}{\Omega_j} e^{-(\Psi_j \kappa \gamma / (\Omega_j (a_4 \Psi_j^2 \kappa^2 - b_4 \Psi_j \kappa \gamma - \Psi_i \gamma))) - (\kappa/\Omega_j)},$$

$$\chi_2(\kappa) = \frac{1}{\Omega_i} e^{-(\kappa/\Omega_i)} - \frac{1}{\Omega_i} e^{-(b_4 \Psi_i \kappa^2 \gamma + \Psi_i \gamma \kappa) / (\Omega_i (a_4 \Psi_i \Psi_j \kappa^2 - \Psi_j \gamma)) - (\kappa/\Omega_i)},$$

$$m_i = \frac{\Omega_i}{\Omega_i + \Omega_j}, m_j = \frac{\Omega_j}{\Omega_i + \Omega_j}, \quad K_1 = \frac{b_4 \gamma + \sqrt{(b_4 \gamma)^2 + 4a_4 \Psi_j \gamma}}{2a_4 \Psi_i}, K_2 = \sqrt{\frac{\gamma}{a_4 \Psi_j}}, \quad K_3 = \frac{b_4 \gamma + \sqrt{(b_4 \gamma)^2 + 4a_4 \gamma (\Psi_i + \Psi_j)}}{2a_4 \Psi_i}, \quad \text{and}$$

$$K_4 = \frac{b_4 \Psi_j \gamma + \sqrt{(b_4 \Psi_j \gamma)^2 + 4a_4 \Psi_i \Psi_j \gamma (\Psi_i + \Psi_j)}}{2a_4 \Psi_i \Psi_j}.$$

(ii) Outage probability:

Lemma 9: The joint distribution function of $F_{\gamma_A^{\text{MRC}}, \gamma_B^{\text{MRC}}}$ for the SBS policy in the TDBC protocol can be expressed as

$$F_{\gamma_A^{\text{MRC}}, \gamma_B^{\text{MRC}}}(Y_A, Y_B) = \int_0^{\min\{(Y_A/\Psi_A), (Y_B/\Psi_B)\}} F_{\gamma_A, \gamma_B}(Y_A - \Psi_B z, Y_B - \Psi_A z) \frac{e^{-(z/\Omega_C)}}{\Omega_C} dz, \quad (61)$$

where F_{γ_A, γ_B} is provided in Appendix 3, with interchanging the parameters $a_5 \rightarrow a_4$ and $b_5 \rightarrow b_4$.

Using Lemmas 8 and 9, following (15), the outage probability of the SBS policy for TDBC is given by

$$P_{\text{out}}^{\text{SBS-TDBC}} = P_{\text{out}}^A + P_{\text{out}}^B - P_{\text{out}}^{AB}, \quad (62)$$

where $P_{\text{out}}^A \triangleq F_{\gamma_A^{\text{MRC}}}(\gamma_A^0)$, $P_{\text{out}}^B \triangleq F_{\gamma_B^{\text{MRC}}}(\gamma_B^0)$, and $P_{\text{out}}^{AB} \triangleq F_{\gamma_A^{\text{MRC}}, \gamma_B^{\text{MRC}}}(\gamma_A^0, \gamma_B^0)$. Here, $F_{\gamma_A^{\text{MRC}}}(\gamma_A^0)$ and $F_{\gamma_B^{\text{MRC}}}(\gamma_B^0)$ are given in (60), and $F_{\gamma_A^{\text{MRC}}, \gamma_B^{\text{MRC}}}(\gamma_A^0, \gamma_B^0)$ is given in (61).

(iii) Throughput analysis:

(a) *Delay-limited transmission:* In this mode, the expression for the throughput is the same as (28), where $P_{\text{out}}^A \triangleq F_{\gamma_A^{\text{MRC}}}(\gamma_A^0)$ and $P_{\text{out}}^B \triangleq F_{\gamma_B^{\text{MRC}}}(\gamma_B^0)$, $F_{\gamma_A^{\text{MRC}}}(\gamma_A^0)$ and $F_{\gamma_B^{\text{MRC}}}(\gamma_B^0)$ are given in (60).

(b) *Delay-tolerant transmission:* In this mode, similar to (29), the throughput is calculated using (48), where $F_{\gamma_A^{\text{MRC}}}(\lambda)$ and $F_{\gamma_B^{\text{MRC}}}(\lambda)$ are given in (60).

(iv) *System energy efficiency:* As suggested in Section 3.1(iv), based on the throughput analysis in Section 3.6(iii), the system energy efficiency for the SBS policy and the TDBC protocol is expressed as

$$\bar{\eta}_{\Phi}^{EE} = \frac{\tau_{\Phi}}{P_k \alpha + (1/3)(P_A + P_B)(1 - \alpha)}. \quad (63)$$

4 Numerical results

In this section, numerical results are presented to illustrate performance including outage probability, throughput and system energy efficiency for different wireless power transfer policies in the EH phase and different transmission protocols in the IP phase. We assume that the co-ordinates of the relay (R), the sources (A), and (B) are (1;0.5), (0;0), and (2;0), respectively. Hence, the distances are calculated as $d_{AR} = \sqrt{5}/2$, $d_{BR} = \sqrt{5}/2$, and $d_{AB} = 2$. In the simulations, without any loss of generality, we assume

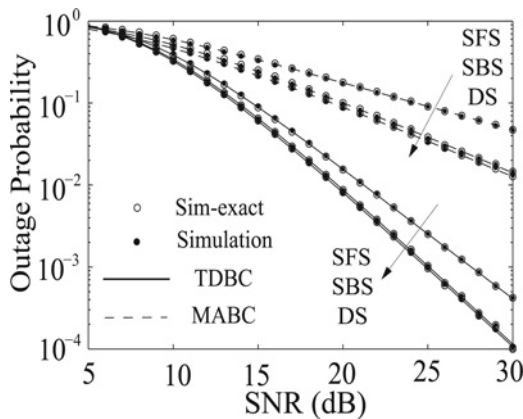


Fig. 2 Outage probability with $\alpha = 0.5$, $\eta = 0.8$, $d_{AR} = \sqrt{5}/2$, $d_{BR} = \sqrt{5}/2$, and $d_{AB} = 2$

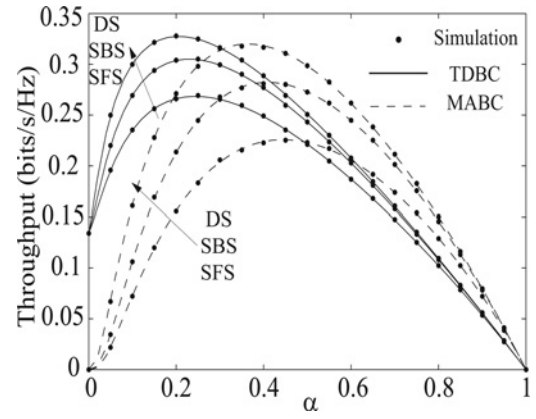


Fig. 3 Throughput in delay-limited transmission mode with $\text{SNR} = 10$ dB, $\eta = 0.8$, $d_{AR} = \sqrt{5}/2$, $d_{BR} = \sqrt{5}/2$, and $d_{AB} = 2$

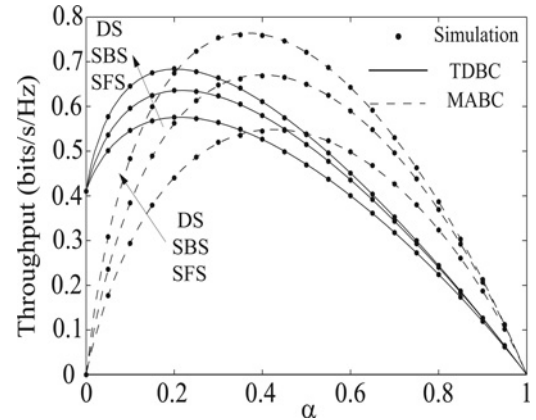


Fig. 4 Throughput in delay-tolerant transmission mode with $\text{SNR} = 10$ dB, $\eta = 0.8$, $d_{AR} = \sqrt{5}/2$, $d_{BR} = \sqrt{5}/2$, and $d_{AB} = 2$

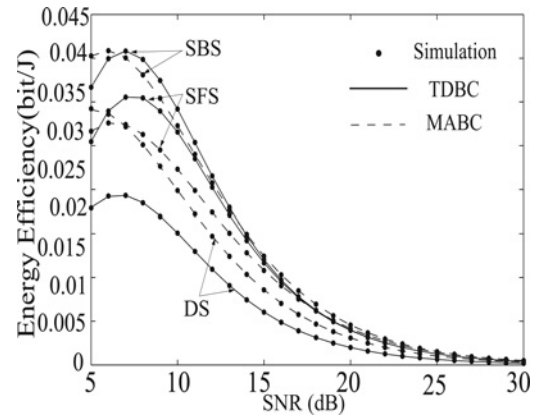


Fig. 5 System energy efficiency in delay-limited transmission mode with $\alpha = 0.5$, $\eta = 0.8$, $d_{AR} = \sqrt{5}/2$, $d_{BR} = \sqrt{5}/2$, and $d_{AB} = 2$

frequency dependent constant $K=1$. We also set the path-loss exponent $\zeta=4$, the threshold value $\gamma_A^0 = \gamma_B^0 = 0$ dB. We assume identical source transmit power at A and B with $P_A = P_B = P$ for simplicity and $\text{SNR} = (P/\sigma^2)$. In the figures, the solid curves represent the TDBC protocol and the dashed curves represent the MABC protocol. We mark the Monte Carlo simulation points for all cases with 'filled circle'. In each figure, we see the precise agreement between the Monte Carlo simulation points and the analytical curves.

Fig. 2 plots the outage probability against SNR. We can observe the approximations have a good match with the exact simulation curves. It is shown that the TDBC protocol achieves lower outage

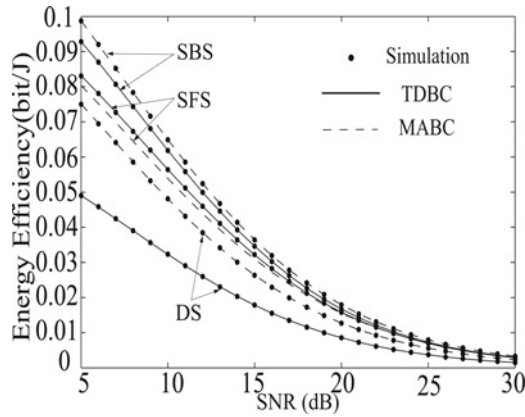


Fig. 6 System energy efficiency in delay-tolerant transmission mode with $\alpha = 0.5$, $\eta = 0.8$, $d_{AR} = \sqrt{5}/2$, $d_{BR} = \sqrt{5}/2$, and $d_{AB} = 2$

probability than the MABC protocol, since the TDBC applies MRC technique to achieve larger diversity gain. For the MABC protocol, we see that the DS policy achieves the lowest outage probability, since it transfers the largest power to the relay. For the TDBC protocol, we see that the achievable outage probability of the proposed policies is still $DS > SBS > SFS$. However, it is worth noting that the SBS policy performs almost identically as the DS policy both in the MABC and the TDBC protocols.

Figs. 3 and 4 plot the throughput against α in delay-limited and in delay-tolerant transmission modes, respectively. Several observations are drawn: (i) in both transmission modes, as α increases, the throughput first increases and then decreases. This is because increasing α means the relay receives more power, but less time for information transmission. Hence there exists an optimal value which provides a tradeoff between power transfer and information transmission; (ii) in both transmission modes, for small α , TDBC achieves higher throughput, by applying MRC to obtain the diversity gain. For large α , MABC performs better than TDBC due to its higher spectrum efficiency; and (iii) in the delay-limited transmission mode, for each power transfer policy, the optimal value of TDBC achieves higher throughput than that of MABC. This is due to the fact that in this mode the throughput is determined by the outage probability and TDBC achieves the lowest outage probability.

Figs. 5 and 6 plot the system energy efficiency against SNR in delay-limited transmission mode and in delay-tolerant transmission mode, respectively. One can observe is that the energy efficiency of the proposed policies in these two modes is $SBS > SFS > DS$ in both the MABC and TDBC protocols. It can be seen that the MABC protocol achieves higher energy efficiency than the TDBC protocol in delay-tolerant mode. It is worth noting that for the SFS policy, the MABC and the TDBC have almost the same system energy efficiency.

Comparing the three proposed power transfer policies from Figs. 2–6. Some observations are concluded as follows: (i) DS policy performs the best in terms of outage probability and throughput but consumes the most energy; (ii) SBS is the most energy efficient policy, but demands instantaneous feedback information; and (iii) SFS policy has the lowest system implementation complexity, but performs the worst in terms of outage probability and throughput. Therefore, it is of importance to select a proper policy according to the practical scenario based on our analysis and numerical results.

5 Conclusions

In this paper, AF TWRNs with an energy constrained relay node harvesting energy by wireless power transfer was considered. We proposed three wireless power transfer policies and considered multiple access broadcasting and time division broadcasting protocols. New outage probability expressions for different power

transfer policies and different transmission protocols were derived to determine the system reliability. From the perspective of delay-limited and delay-tolerant transmission modes, the throughput and energy efficiency were examined. Numerical results were presented to verify the analysis and provided useful insights into the practical design of the considered networks.

6 Acknowledgments

This work was supported by the Newton Institutional Link under Grant ID 172719890.

7 References

- 1 Liu, V., Parks, A., Talla, V., *et al.*: 'Ambient backscatter: wireless communication out of thin air'. Proc. ACM SIGCOMM, 2013, pp. 39–50
- 2 Brown, W.C.: 'The history of power transmission by radio waves', *IEEE Trans. Microw. Theory Techn.*, 1984, **32**, (9), pp. 1230–1242
- 3 Varshney, L.: 'Transporting information and energy simultaneously'. Proc. IEEE Int. Symp. on Information Theory (ISIT), 2008, pp. 1612–1616
- 4 Zhang, R., Ho, C.K.: 'MIMO broadcasting for simultaneous wireless information and power transfer', *IEEE Trans. Commun.*, 2013, **12**, (5), pp. 1989–2001
- 5 Xiang, Z., Tao, M.: 'Robust beamforming for wireless information and power transmission', *IEEE Wirel. Commun. Lett.*, 2012, **1**, (4), pp. 372–375
- 6 Liu, Y., Wang, L., Zaidi, S., *et al.*: 'Secure D2D communication in large-scale cognitive cellular networks: a wireless power transfer model', *IEEE Trans. Commun.*, 2016, **64**, (1), pp. 329–342
- 7 Qin, Z., Liu, Y., Gao, Y., *et al.*: 'Throughput analysis of wireless powered cognitive radio networks with compressive sensing and matrix completion', 2016. Available at: <http://www.arxiv.org/abs/1601.06578>
- 8 Liu, L., Zhang, R., Chua, K.-C.: 'Wireless information and power transfer: a dynamic power splitting approach', *IEEE Trans. Commun.*, 2013, **61**, (9), pp. 3990–4001
- 9 Nasir, A.A., Zhou, X., Durrani, S., *et al.*: 'Relaying protocols for wireless energy harvesting and information processing', *IEEE Trans. Wirel. Commun.*, 2013, **12**, (7), pp. 3622–3636
- 10 Liu, Y., Mousavifar, S., Deng, Y., *et al.*: 'Wireless energy harvesting in a cognitive relay network', *IEEE Trans. Wirel. Commun.*, 2016, **15**, (4), pp. 2498–2508
- 11 Liu, Y., Ding, Z., Elkashlan, M., *et al.*: 'Cooperative non-orthogonal multiple access with simultaneous wireless information and power transfer', *IEEE J. Sel. Areas Commun.*, 2016, **34**, (4), pp. 938–953. Available at: <http://www.arxiv.org/abs/1511.02833>
- 12 Rankov, B., Wittneben, A.: 'Spectral efficient protocols for half-duplex fading relay channels', *IEEE J. Sel. Areas Commun.*, 2007, **25**, (2), pp. 379–389
- 13 Wang, R., Tao, M.: 'Outage performance analysis of two-way relay system with multi-antenna relay node'. Proc. IEEE Int. Conf. Communications (ICC), 2012, pp. 3538–3542
- 14 Chen, Z., Xia, B., Liu, H.: 'Wireless information and power transfer in two-way amplify-and-forward relaying channels'. Proc. IEEE Global Conf. on Signal and Information Processing (GlobalSIP), 2014, pp. 168–172
- 15 Liu, Y., Wang, L., Elkashlan, M., *et al.*: 'Two-way relaying networks with wireless power transfer: Policies design and throughput analysis'. Proc. IEEE Global Communication Conf. (GLOBECOM), 2014, pp. 4030–4035
- 16 Zhou, X., Zhang, R., Ho, C.K.: 'Wireless information and power transfer: Architecture design and rate-energy tradeoff'. Proc. IEEE Global Communication Conf. (GLOBECOM), 2012, pp. 3982–3987
- 17 Hasna, M.O., Alouini, M.-S.: 'End-to-end performance of transmission systems with relays over Rayleigh-fading channels', *IEEE Trans. Wirel. Commun.*, 2003, **2**, (6), pp. 1126–1131
- 18 Gradshteyn, I.S., Ryzhik, I.M.: 'Table of integrals, series and products' (Academic Press, New York, NY, USA, 2000, 6th edn.)

8 Appendices

8.1 Appendix 1

The joint distribution function of F_{γ_A, γ_B} for the DS policy in the MABC protocol is calculated as (see equation (64) at the bottom of the next page)

$$\text{where } K_i^0 = \left(\beta_i + \sqrt{\beta_i^2 + 4\varpi_j Y_j (Y_i)^2 \vartheta^2} \right) / 2\varpi_j Y_i \vartheta \quad \text{with} \\ \beta_i = \vartheta^2 Y_j Y_i + \varpi_i Y_j - \varpi_j Y_i, (i, j) \in \{(A, B), (B, A)\}.$$

8.2 Appendix 2

The joint distribution function of F_{γ_A, γ_B} for the SFS policy in the MABC protocol is calculated as follows (see equation (65) at the bottom of the next page)

where

$$\begin{aligned}\Delta_1 &= a_2 \Psi_A^2 X^2 - b_2 \Psi_A X Y_A - \Psi_B Y_A, \\ \Delta_2 &= a_2 \Psi_A \Psi_B X^2 - Y_B \Psi_B, \\ \varphi_1(x) &= \frac{1}{\Omega_A} e^{-(x/\Omega_A)} \\ &\quad - \frac{1}{\Omega_A} e^{-((\Psi_A X Y_A)/(\Omega_B(a_2 \Psi_A^2 X^2 - b_2 \Psi_A X Y_A - \Psi_B Y_A)) - (x/\Omega_A))}, \\ \varphi_2(x) &= \frac{1}{\Omega_A} e^{-(x/\Omega_A)} \\ &\quad - \frac{1}{\Omega_A} e^{-((Y_B b_2 \Psi_A X^2 + Y_B \Psi_A X)/(\Omega_B(a_2 \Psi_A \Psi_B X^2 - Y_B \Psi_B)) - (x/\Omega_A))}, \\ X_1 &= \frac{b_2 Y_A + \sqrt{(b_2 Y_A)^2 + 4a_2 \Psi_B Y_A}}{2a_2 \Psi_A}, \quad X_2 = \sqrt{\frac{Y_B}{a_2 \Psi_A}}, \quad \text{and} \\ X_0 &= \frac{\beta_2 + \sqrt{(\beta_2)^2 + 4a_2 b_2^2 \Psi_A^2 Y_A (Y_B)^2 (\Psi_A + \Psi_B)}}{2ab Y_B \Psi_A^2}, \quad \text{with} \\ \beta_2 &= a_2 \Psi_A \Psi_B Y_A + b_2^2 \Psi_A Y_A Y_B - a \Psi_A^2 Y_B.\end{aligned}$$

8.3 Appendix 3

The joint distribution function of F_{γ_A, γ_B} for the SBS policy in the MABC protocol is calculated as follows: (see (66))

where $\Delta_{x1} = a_4 \Psi_A^2 X^2 - b_4 \Psi_A X Y_A - \Psi_B Y_A$, $\Delta_{x2} = a_4 \Psi_A \Psi_B X^2 - \Psi_B Y_B$, $\Delta_{y1} = a_4 \Psi_B^2 Y^2 - b_4 \Psi_B Y Y_A - \Psi_A Y_A$, $\Delta_{y2} = a_4 \Psi_A \Psi_B Y^2 - \Psi_A Y_B$

$$\begin{aligned}\phi_1(\kappa) &= \frac{1}{\Omega_i} e^{-(\kappa/\Omega_i)} - \frac{1}{\Omega_i} e^{-((\Psi_i \kappa Y_i)/(\Omega_j(a_4 \Psi_i^2 \kappa^2 - b_4 \Psi_i \kappa Y_i - \Psi_j Y_j))) - (\kappa/\Omega_i)}, \\ \phi_2(\kappa) &= \frac{1}{\Omega_i} e^{-(\kappa/\Omega_i)} \\ &\quad - \frac{1}{\Omega_i} e^{-((b_4 \Psi_i \kappa^2 Y_j + \Psi_i Y_j \kappa)/(\Omega_j(a_4 \Psi_i \Psi_j \kappa^2 - \Psi_j Y_j))) - (\kappa/\Omega_i)}, \\ m_i &= \frac{\Omega_i}{\Omega_i + \Omega_j}, \quad m_j = \frac{\Omega_j}{\Omega_i + \Omega_j}, \\ \Theta_1 &= U(K_0 - \max\{K_1, K_2, K_4\}), \\ \Theta_2 &= U(\min\{K_3, K_4\} - \max\{K_1, K_2\}), \\ \Theta_3 &= U(K_1 - \max\{K_2, K_4\}), \\ \Theta_4 &= U(\min\{K_1, K_4\} - K_2), \quad \Theta_5 = U(K_2 - \max\{K_1, K_3\}), \\ \Theta_6 &= U(\min\{K_2, K_3\} - K_1), \\ K_0 &= \left(\beta + \sqrt{\beta^2 + 4a_4 b_4^2 \Psi_i^2 Y_i (Y_j)^2 (\Psi_i + \Psi_j)} \right) / 2a_4 b_4 Y_j \Psi_i^2, \\ \beta &= a_4 \Psi_i \Psi_j Y_i + b_4^2 \Psi_i Y_i Y_j - a_4 \Psi_i^2 Y_j, \\ K_1 &= \frac{b_4 Y_i + \sqrt{(b_4 Y_i)^2 + 4a_4 \Psi_j Y_i}}{2a_4 \Psi_i}, \quad K_2 = \sqrt{\frac{Y_j}{a_4 \Psi_i}} \\ K_3 &= \frac{b_4 Y_i + \sqrt{(b_4 Y_i)^2 + 4a_4 Y_i (\Psi_j + \Psi_i)}}{2a_4 \Psi_i}, \quad \text{and} \\ K_4 &= \frac{b_4 \Psi_i Y_j + \sqrt{(b_4 \Psi_i Y_j)^2 + 4a_4 \Psi_i \Psi_j Y_j (\Psi_i + \Psi_j)}}{2a_4 \Psi_i \Psi_j}.\end{aligned}$$

$$\begin{aligned}F_{\gamma_A, \gamma_B}(Y_A, Y_B) &= \Pr(\gamma_A < Y_A, \gamma_B < Y_B) = \Pr\left(Y \leq \frac{Y_A(\partial X + 1)}{\Psi_A X}, \quad X \leq \frac{Y_B(\partial Y + 1)}{\Psi_B Y}\right) \\ &= \int_0^{K_A^0} \int_{(K_B^0/K_A^0)X}^{(Y_A(\partial x + 1)/\Psi_A X)} \frac{e^{-(x/\Omega_A) - (y/\Omega_B)}}{\Omega_A \Omega_B} dy dx + \int_0^{K_B^0} \int_{(K_A^0/K_B^0)Y}^{(Y_B(\partial y + 1)/\Psi_B Y)} \frac{e^{-(x/\Omega_A) - (y/\Omega_B)}}{\Omega_A \Omega_B} dx dy \\ &= 1 - e^{-(K_A^0/\Omega_A) - (K_B^0/\Omega_B)} - \sum_{\substack{i,j \in \{A,B\} \\ i \neq j}} \frac{e^{-(Y_j \partial/\partial \Omega_i)}}{\Omega_j} \int_0^{K_i^0} \left(e^{-(Y_j/\Psi_j \Omega_i \kappa) - (\kappa/\Omega_j)} \right) d\kappa,\end{aligned}\quad (64)$$

$$\begin{aligned}F_{\gamma_A, \gamma_B}(Y_A, Y_B) &= \Pr(\gamma_A < Y_A, \gamma_B < Y_B) = \Pr[Y \Delta_1 \leq \Psi_A X Y_A, Y \Delta_2 \leq Y_B X \Psi_A (b_2 X^2 + 1)] = 1 - e^{-(\min\{X_1, X_2\}/\Omega_A)} \\ &\quad + \int_{\max\{X_0, X_1, X_2\}}^{\infty} \varphi_1(x) dx + U(X_0 - \max\{X_1, X_2\}) \int_{\max\{X_1, X_2\}}^{X_0} \varphi_2(x) dx + U(X_2 - X_1) \int_{X_1}^{X_2} \varphi_1(x) dx + U(X_1 - X_2) \int_{X_2}^{X_1} \varphi_2(x) dx,\end{aligned}\quad (65)$$

$$\begin{aligned}F_{\gamma_A, \gamma_B}(Y_A, Y_B) &= \Pr(\gamma_A < Y_A, \gamma_B < Y_B) = \Pr[Y \Delta_{x1} \leq \Psi_A X Y_A, Y \Delta_{x2} \leq \Psi_A Y_B X (b_4 X + 1), X \geq Y] \\ &\quad + \Pr[X \Delta_{y1} \leq \Psi_B Y Y_A, X \Delta_{y2} \leq \Psi_B Y_B Y (b_4 Y + 1), X < Y] = \sum_{\substack{i,j \in \{A,B\} \\ i \neq j}} \left(\int_{\max\{K_0, K_1, K_2, K_3\}}^{\infty} \phi_1(\kappa) d\kappa + \Theta_1 \int_{\max\{K_1, K_2, K_4\}}^{K_0} \phi_2(\kappa) d\kappa \right. \\ &\quad + \Theta_2 \left(e^{-(\max\{K_1, K_2\}/\Omega_j)} - e^{-(\min\{K_3, K_4\}/\Omega_j)} - m_i \left(e^{-(\max\{K_1, K_2\}/m_i \Omega_j)} - e^{-(\min\{K_3, K_4\}/m_i \Omega_j)} \right) \right) \\ &\quad + \Theta_3 \int_{\max\{K_2, K_4\}}^{K_1} \phi_2(\kappa) d\kappa + \Theta_4 \left(e^{-(K_2/\Omega_j)} - e^{-(\min\{K_1, K_4\}/\Omega_j)} - m_i \left(e^{-(K_2/m_i \Omega_j)} - e^{-(\min\{K_1, K_4\}/m_i \Omega_j)} \right) \right) \\ &\quad + \Theta_5 \int_{\max\{K_1, K_3\}}^{K_2} \phi_1(\kappa) d\kappa + \Theta_6 \left(e^{-(K_1/\Omega_j)} - e^{-(\min\{K_2, K_3\}/\Omega_j)} - m_i \left(e^{-(K_1/m_i \Omega_j)} - e^{-(\min\{K_2, K_3\}/m_i \Omega_j)} \right) \right) \\ &\quad \left. + 1 - e^{-(\min\{K_1, K_2\}/\Omega_j)} - m_i \left(1 - e^{-(\min\{K_1, K_2\}/m_i \Omega_j)} \right) \right),\end{aligned}\quad (66)$$